Plasmonics
https://doi.org/10.1007/s11468-024-02429-8

RESEARCH

High-Performance Plasmonic Biosensor for Blood Cancer Detection: Achieving Ultrahigh Figure-of-Merit

Yashaswini Singh[1] · Adarsh Chandra Mishra[1] · Sapana Yadav[1] · Laxmi Jaiswal[1] · Pooja Lohia[2] · D. K. Dwivedi[1] · R. K. Yadav[3] · Gaber E. Eldesoky[4] · M. Khalid Hossain[5]

Received: 19 May 2024 / Accepted: 15 July 2024

Abstract

A highly sensitive hybrid structure for biosensing application based on surface plasmon resonance for the detection of blood cancer has been proposed in this article. The biosensor comprises of a CaF_2 Prism, Ag metal, an oxide layer Al_2O_3 and a 2D nanomaterial graphene, which is grounded on Kretschmann configuration. The transfer matrix method is used to interrogate the performance parameters of proposed biosensor. To analyze the change in refractive index, the analyte has been considered over the graphene layer. To achieve maximum sensitivity and minimum reflectance the thickness of Ag, Al_2O_3 layers and number of graphene layers have been optimized. The suggested structure's sensitivity can be enhanced up to 427.43 deg/RIU with the optimized value for the detection accuracy and FOM of 0.7027 deg^{-1} and 217 RIU^{-1} respectively. The work focuses on the development of plasmonic sensors with high performance and stability. Role of different material layers is also analyzed in terms of enhancement in sensitivity and evanescent field. The paper offers better optimization technique and selection of material than previously reported works, which eventually leads to enhancement in both sensitivity and FOM. This research could lead to the development of a useful biological sample sensing tool for the quick and precise detection of the blood cancer in its early stages.

Keywords Blood cancer · Plasmon · Heterostructure · Figure-of-merit

Introduction

Over the past two decades, researchers have closely inspected surface plasmon resonance (SPR) technology because of its capacity to address a broad spectrum of real-time challenges, especially in the biomedical domain [1, 2]. In recent years, SPR-based sensing technology has made remarkable progress in identifying glucose labels, characterizing antibodies, detecting cancer cells, and facilitating DNA hybridization [2, 3]. Furthermore, the exploration of food and environmental samples, along with the detection and characterization of biomolecules and biochemicals, holds promising prospects for SPR-based biosensors. Researchers are more interested in biosensors based on SPR technology because of their strong label-free and real-time sensing capabilities [4–7]. Because of its extraordinary high sensitivity, biocompatibility, detection accuracy, and other features, SPR biosensors are becoming more and more common. Their remarkable reutilization performance and reproducibility, coupled with quantitative analysis for toxicity risk management and dosage control, are the reasons behind their success [8–11]. SPR sensors also make it possible to measure the kinetics and affinity of biomolecular binding in real time. A thin metal film with plasmon resonance properties that is extremely sensitive to changes in refractive index (RI) close to its surface is frequently employed for developing SPR sensors.

✉ D. K. Dwivedi
todkdwivedi@gmail.com

1 Photonics and Photovoltaic Research Lab (PPRL), Department of Physics and Material Science, Madan Malaviya University of Technology, Gorakhpur, India 273010

2 Department of Electronics and Communication Engineering, Madan Mohan Malaviya University of Technology, Gorakhpur, India 273010

3 Department of Chemistry and Environmental Science, Madan Mohan Malaviya University of Technology, Gorakhpur, India 273010

4 Department of Chemistry, College of Science, King Saud University, P.O. Box 2455, 11451 Riyadh, Saudi Arabia

5 Institute of Electronics, Atomic Energy Research Establishment, Bangladesh Atomic Energy Commission, Dhaka 1349, Bangladesh

Published online: 27 July 2024

This arises from the surface plasmon wave generating a strong evanescent field at the metal–dielectric interface [12, 13]. The plasmonic signal is altered as a result of analyte adsorption on the metal surface. The most popular prism based SPR arrangement is the Kretschmann setup. When p-polarized light is incident upon a thin metallic film, free electrons on the metal surface will excite and produce a surface plasmon through the prism. As the surface plasmon resonates by absorbing the energy of incident light, the intensity of the reflected light diminishes. The particular incident angle at which the reflection intensity is minimum, is called resonance angle [14–16].

The two main methods of detection in SPR sensors with a Kretschmann configuration are angular interrogation and wavelength interrogation. The angular interrogation uses monochromatic light and yields higher signal-to-noise ratios because the source's power and wavelength are more stable [17]. The typical SPR biosensors consist of a plasmonic metal layer and a glass prism. The prism couples the surface plasmon which is propagating along the metal–dielectric interface, with the wave vector of incoming light. For the analysis of small amounts of analyte, these traditional SPR-based sensors fail to maximize performance [18]. The limitation of traditional SPR sensors presents a chance for researchers to create multilayer SPR sensors and incorporate diverse 2D nanomaterials, perovskite materials, plasmonic materials and semiconductor materials to significantly improve the accuracy of SPR sensors [19, 20].

Prisms with a lower RI are observed to perform better and have higher sensitivity when compared, which is the foundation for the prism selection. In SPR sensors, metal films such as silver (Ag), aluminum (Al), gold (Au), copper (Cu) etc., are frequently employed [21–24]. Among SPR sensors, Au is unique due to its remarkable stability and bioactivity. However, utilization of gold in this instance causes a wider SPR curve, which compromises the sensitivity of the sensor. Because of its narrower resonance peak, which increases the detection accuracy of the SPR sensor, Ag performs better in SPR sensors than Au. Nevertheless, oxidation and corrosion are major drawbacks of Ag film [25]. To solve these issues, bimetallic layers and metal oxides (TiO_2 [26], ZnO [27], Al_2O_3 [28]etc.) can be implemented, which may also improve the sensitivity of the sensor. For the proposed sensor, semiconductor materials are considered more suitable due to their additional properties like high surface-to-volume ratio, chemical stability, and molecular binding ability. The existence of a bimetallic layer strengthens the sensor's sensitivity because even small fluctuations in the RI of analyte lead to significant shifts in the SPR angle [29–31].

2D nanomaterials have been gaining a lot of attention nowadays, because of their remarkable chemical and physical properties. These materials feature strong in-plane bonds and weaker bonds out-of-plane [32, 33]. The increased surface-to-volume ratio in 2D materials provides a multitude of binding sites for biological specimens, leading to significantly altered light signals and improved sensor functionality. Graphene is a good example of a material with an ultrathin structure and a high specific surface area ratio, which provides a lot of active sites for molecular interactions. Furthermore, when designing plasmonic sensors, researchers have a great deal of flexibility because of graphene's optical properties, which change with layer thickness. Furthermore, considering graphene's strong chemical and thermal stability, it can serve as a shield for metallic nanoparticles [34, 35]. Graphene is a promising material that could see widespread use in biomedical sensing applications due to its remarkable biocompatibility. Also, the effective use of graphene has encouraged research into a number of other 2D nanomaterials, including transition. A strong coupling is observed at the metal interface upon the deposition of graphene onto a metal film. The efficient charge transfer between the layers of sensor heterostructure becomes feasible by the high carrier mobility of 2D nanomaterials [36, 37].

Cancer, characterized by the unregulated growth of abnormal cells in a particular region of the body, stands as one of the leading causes of mortality worldwide. Thus, timely diagnosis of these ailments becomes crucial [38, 39]. SPR technique is one of the best methods for its detection. The article demonstrates the development of an SPR-based optical sensor for quick detection of blood cancer. This research encompasses developing a theoretical design of an SPR biosensor using angular interrogation, employing the transfer matrix method (TMM) [40]. CaF_2 prism has been used as coupling prism while Ag is utilized as plasmonic metal. Further, Al_2O_3 and graphene are also used to enhance the performance of the sensor in terms of sensitivity. To achieve optimum performance the number of layers and thicknesses for each layer is varied. The performance of the sensor is evaluated in terms of sensitivity and figure-of-merit (FOM).

Design Consideration and Theoretical Modeling

Sensor Design and Materials

The schematic diagram of the proposed multilayer biosensor set up in a standard Kretschmann configuration, is shown in Fig. 1(a). This structure consists of six layers organized as CaF_2/Ag/Al_2O_3/Ag/graphene/analyte. A source of light with wavelength 633 nm is chosen as the operating wavelength. Figure 1(b) is electric field plot for the proposed sensor structure. It shows the existence of evanescent field in the ambient region which consequently confirms the existence of plasmons and validity of the

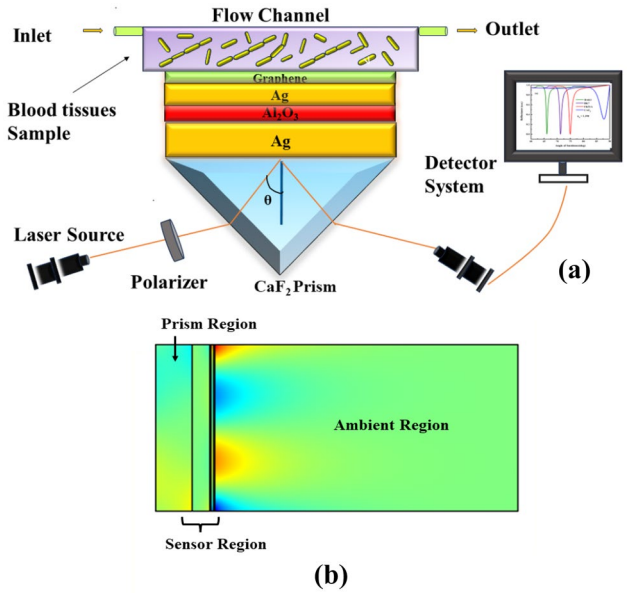

Fig. 1 **a** Proposed SPR sensor structure for blood cancer detection and **b** encroaching evanescent field in the ambient region for the proposed structure

structure as SPR sensor. The first layer is made of CaF_2 glass which serves as the prism. This article enhances setup with superior angular error rejection through the utilization of a CaF_2 prism as the coupling substrate, capitalizing on its low RI. Moreover, the low RI of this substrate significantly heightens the biosensor's angular sensitivity and induces a shift in the reflectance curve compared to an alternative prism. The RI of the CaF_2 prism is determined using the Sellmeier equation as given below [41]

$$n^2_{\mathrm{CaF2}} = \left(\mathrm{a} + \frac{\mathrm{b}\times\lambda^2}{\lambda^2 - c^2} + \frac{\mathrm{d}\times\lambda^2}{\lambda^2 - f^2} + \frac{\mathrm{g}\times\lambda^2}{\lambda^2 - h^2}\right) \tag{1}$$

where $a=1.33973$, $b=0.69913$, $c=0.09374$, $d=0.11994$, $f=21.18$, $g=4.35181$, $h=38.46$, and λ is wavelength of incident electromagnetic wave. Through a physical deposition technique, a precise thickness Ag metal film can be deposited on the prism base. Among the considered metal layers, Ag notably contributes to the narrower resonance curve and higher sensitivity. Utilizing the Drude Lorentz model the complex RI of Ag can be given as below [41, 42]

$$n^2_{Ag} = \varepsilon_{Ag} = \left(1 - \frac{\lambda_c \times \lambda^2}{\lambda_p^2(\lambda_c + i\lambda}\right) \tag{2}$$

In this instance, the collision and plasma wavelengths are represented by λ_c and λ_p, which have respective values of 1.7914×10^{-5} m and 1.4541×10^{-7} m. After the metal-dielectric (prism) interface forms, surface plasmons arise and then propagate along the surface. Unfortunately, the biosensor's lifespan is shortened due to the oxidation of the Ag layer. To address the significant issue of lifespan reduction due to oxidation of the Ag layer Al_2O_3 has been deposited over Ag. As a metal oxide with good conductivity, it shifts the functional wavelength toward the near-infrared spectrum. Additional advantageous qualities for the SPR biosensor include enhanced electrochemical stability, non-toxicity, lower carrier concentration (approximately 10^{20}–10^{22}/cm^2), and resistance to corrosion mechanisms.

The dispersion formula furnishes the RI value of Al_2O_3 at a wavelength of 633 nm, and it is expressed as [43]:

$$n^2_{Al203} = 1 + \frac{1.43134936\lambda^2}{\lambda^2 - (0.0726631)^2} + \frac{0.65054713\lambda^2}{\lambda^2 - (0.1193242)^2} + \frac{5.3414021\lambda^2}{\lambda^2 - (18.028251)^2} \tag{3}$$

Now, to improve the performance, the fourth layer of the proposed biosensor is again Ag metal which makes it bimetallic sensor. The fifth layer is a monolayer of graphene. Because of its large surface area and enhanced sensitivity to changes in the environment, graphene can detect even very low analyte concentrations and its overall sensing efficiency is improved by this. The sensing medium, also known as the analyte medium, is the final layer. For diagnosis, different samples of blood cancer infected cells. The RI of normal and infected blood cells are 1.376 and 1.390 respectively [38, 44]. Table 1 summarizes RI and thickness variation considered for each layer of the sensor.

Performance Parameters

Several important parameters are utilized to evaluate the performance of SPR sensors. These include sensitivity (S), full width at half maximum (FWHM), quality factor (QF), detection accuracy (DA), and limit of detection (LoD).

Sensitivity

Sensitivity reflects the sensor's capability to detect slight variations in the RI on its surface. If there is a shift of $\Delta\theta_{\mathrm{res}}$ in the angle of SPR due to a variation in Δn in RI, angular sensitivity can be defined as [45]:

$$S = \frac{\Delta\theta res}{\Delta n} \tag{4}$$

Table 1 RI and thickness variation for the proposed sensor structure

Layers	Materials	RI at λ = 633nm	Thickness (in nm)
I	CaF_2	1.4329	–
II	Ag	0.056206 + 4.2776i	30 to 60
III	Al_2O_3	1.7659	0 to 10
IV	Ag	0.056206 + 4.2776i	0 to 30
V	Graphene	3.0 + 1.1487i	0 to 4 (no. of layers)

Full Width at Half Maxima (FWHM)

The FWHM defines the width of a peak when its amplitude equals half of its maximum value on a graph or spectrum. FWHM basically describes the width of the reflectance of power loss spectrum. A lower FWHM value indicates highly resolvable spectrum. It can be expressed as [46]:

$$\text{FWHM} = \frac{1}{2}(\theta_{max} + \theta_{min}) \tag{5}$$

Figure-of-Merit (FOM)

The ratio of sensitivity to FWHM is known as the FOM, or quality factor, and is expressed as [24]:

$$\text{FOM} = \frac{\text{S}}{\text{FWHM}} \tag{6}$$

The power loss for the optimized structure can be obtained from following equation [29]:

$$Power\ loss\ (in\ dB) = 10\log_{10}\frac{1}{R(\theta)} \tag{7}$$

where $R(\theta)$ is normalized reflection coefficient which can be obtained using mathematical formulation using [47].

Fabrication Feasibility and Process

An optimal thickness of Ag metal film can be deposited over the base of CaF_2 prism by using physical deposition techniques (PVD) such as thermal evaporation, spin coating or electro-coating. A thin layer of Al_2O_3 can be grown on the metal surface by chemical vapor deposition (CVD) technique or sol–gel method. Again, using CVD techniques, the graphene layer can be grown on the top of the structure. All the nanoscale layers can also be deposited by using atomic layer deposition (ALD) process due to its low temperature operation and high-quality fabrication.

Result and Discussion

Initially, four sensor designs comprising of CaF_2/Ag/Analyte (conventional), CaF_2/Ag/Al_2O_3/analyte, CaF_2/Ag/Al_2O_3/Ag/analyte, and CaF_2/Ag/Al_2O_3/Ag/graphene/analyte has been considered to analyze their respective sensitivity and identify the most effective design.

Figure 2 depicts the variation in reflectance with angle of incidence. Both the sensitivity and resonance angle shift have been found to increase with design intricacy. The CaF_2/Ag/analyte design, featuring a 45 nm thick Ag layer, exhibits a resonance angle shift of $\Delta\theta = 4.747°$ with a sensitivity of 339 deg/RIU as illustrated in Fig. 2(a). Progressing to Fig. 2(b), the resonance angle shift advances to $\Delta\theta = 5.26°$ with a sensitivity of 376 deg/RIU for the CaF_2/Ag/Al_2O_3/analyte structure with an Al_2O_3 layer thickness of 1 nm. Moreover, the resonance angle shift again enhances to $\Delta\theta = 5.464°$ with a sensitivity of 390 deg/RIU for the CaF_2/Ag/Al_2O_3/Ag/analyte structure, as depicted in Fig. 2(c) which includes an Ag layer thickness of 5 nm. Eventually, utilizing a monolayer of graphene yields a resonance angle shift of $\Delta\theta = 5.83°$ and a sensitivity of 417 deg/RIU. The supremacy of the ultimate configuration, i.e., CaF_2/Ag/Al_2O_3/Ag/graphene/analyte, over all other proposed designs is evident. Therefore, priority will be given to the final structure for further optimization. The values of performance parameters corresponding to Fig. 2 are displayed in Table 2.

It is evident from Table 2 that using bimetallic structure, the sensitivity and FOM can be significantly enhanced compared to single metal layer. Bimetallic thin films exhibit multiple plasmon resonance due to their complex structure. This can broaden the spectral response and increase sensitivity because of stronger near-field enhancement. However, this design is not chemically stable (due to higher oxidation rate of Ag) and efficient toward bio-sample adsorption. To fulfil both requirements, we considered graphene layer at the top of design. The high surface to volume ratio of graphene helps in adsorption of biomolecules and its chemical inert nature can protect the Ag from oxidation.

To effectively couple the wave vector of an incoming photon with that of surface plasmon waves, selection of prism is crucial. To achieve the maximum sensitivity, a prism material is selected based on its low RI and higher angle of resonance simultaneously. A prism with lower RI is also able to provide coupling for higher wavelength regions. Therefore, BK7 (RI = 1.5151), BAK1 (RI = 1.570), FK51A (RI = 1.4853), and CaF2 (RI = 1.4329) prisms have been compared based on their resonance angle and corresponding sensitivity.

Figure 3(a) manifests the reflectance curve for the final structure with blood cancerous tissue serving as the analyte medium. However, across different prism materials, the curve exhibits remarkable absorption dips, with CaF_2 emerging as the most suitable prism material. CaF_2 provides the resonance angle at higher incident angles compared to other prism materials. The corresponding sensitivity for different prism materials is illustrated in Fig. 3(b). The maximum sensitivity of 417 deg/RIU is obtained for the CaF_2-based sensor structure. This transpires because a greater angle of incidence not only generates more surface plasmons but also enhances the effective overlap integral and coupling between reflected light and the approaching evanescent wave toward the surrounding region. Consequently, a perceptible shift in resonance dip

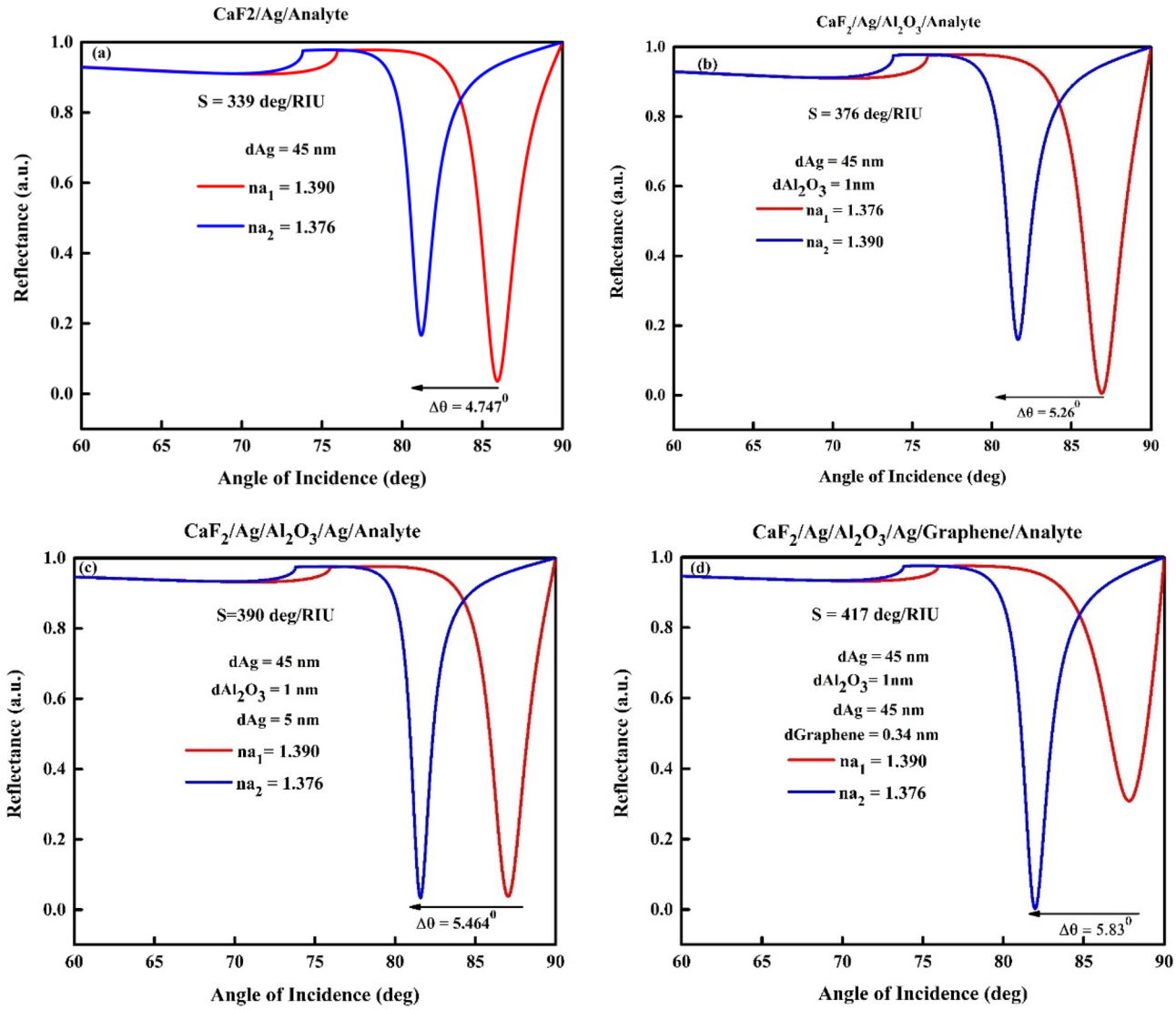

Fig. 2 Variation of reflectance with angle of incidence for **a** CaF_2/Ag/analyte, **b** CaF_2/Ag/Al_2O_3/analyte, **c** CaF_2/Ag/Al_2O_3/Ag/analyte, **d** CaF_2/Ag/Al_2O_3/Ag/graphene/analyte structures

may result from even a small alteration in the RI of sensing medium.

Additionally, for the final design of suggested sensor, the thickness and number of layers have been optimized. The optimization is undertaken with careful prudent analysis of the viability of precisely depositing a 1 nm thick layer of the constituent materials. Upon varying thickness of one layer, thicknesses of all other layers are kept constant.

Figure 4(a) depicts the variation in the thickness of the Ag layer, which ranges from 30 to 60 nm, advancing in increments of 1 nm. The findings pinpoint a peak sensitivity of 427.43 deg/RIU for Ag thickness of 45 nm. on both sides

Table 2 Values of performance parameters corresponding to Fig. 2

Structures	Sensitivity (deg/RIU)	FWHM (deg.)	FOM (RIU^{-1})
CaF_2/Ag/analyte	339	1.8290	185
CaF_2/Ag/Al_2O_3/analyte	376	1.9330	194
CaF_2/Ag/Al_2O_3/Ag/analyte	390	1.4810	263
CaF_2/Ag/Al_2O_3/Ag/graphene/analyte	417	1.9170	217

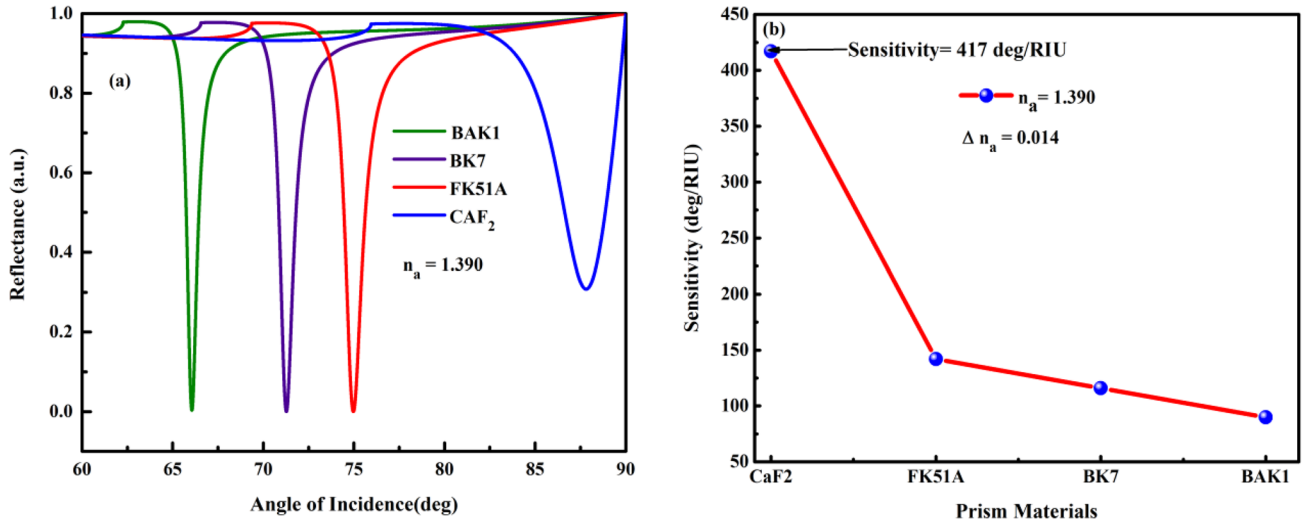

Fig. 3 **a** Variation in reflectance with incident angle for various prism materials, and **b** the corresponding variations in sensitivity for different prism materials

of 45 nm, the sensitivity decreases, which indicates crucial dependence of sensitivity on the thickness of Ag. In a similar vein, Fig. 4(b) demonstrates alterations in the Al_2O_3 thickness, varied between 0 to 10 nm. Here, the highest sensitivity of 427.43 deg/RIU is achieved at Al_2O_3 thickness of 1 nm. The sensitivity sharply decreases on increasing the Al_2O_3 thickness after 1 nm. Likewise, Fig. 4(c) displays variations in the Ag layer thickness from 0 to 30 nm, where the superior sensitivity is attained at the Ag layer of thickness of 23 nm. Figure 5 demonstrates the variation in sensitivity as the number of graphene layer while employing a 45-nm Ag layer, a 1-nm Al_2O_3 layer, and again Ag layer of thickness of 23 nm. The outcomes manifest that the graphene monolayer exhibits a peak shift of 5.84° and an associated sensitivity of 427.43 deg/RIU. It is evident that the sensitivity is the highest for monolayers of graphene and progressively diminishes as the number of layers increases.

Employing the optimized thickness and number of layers, Fig. 5 portrays the power loss (in dB) for normal and cancerous tissues.

The graph showcases a resonance angle shift of 5.84° along with a sensitivity of 427.43 deg/RIU. The FOM value stands impressively high at 217 RIU^{-1}, while the FWHM is minimized to 1.9170. The peak power loss for cancerous tissue is 1.831 dB while that for normal tissue is 7.449 dB providing the power loss ratio (PLR) of 4.068. A high-power loss ratio provides well-resolved detection. Based on that,

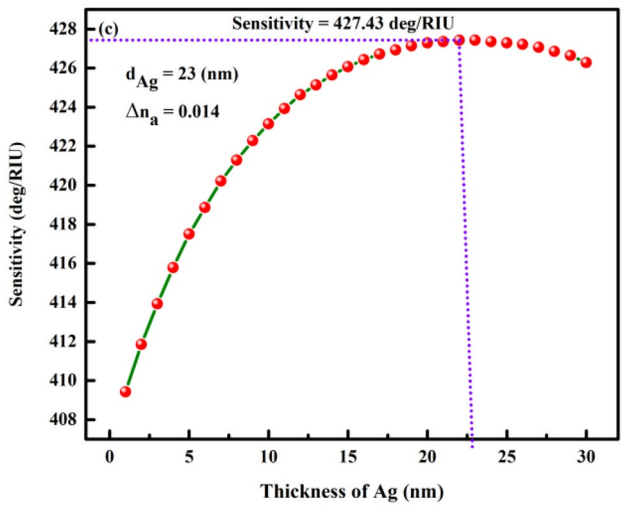

Fig. 4 Variation in Sensitivity concerning with thickness of **a** Ag layer, **b** Al_2O_3 layer, and **c** Ag layer

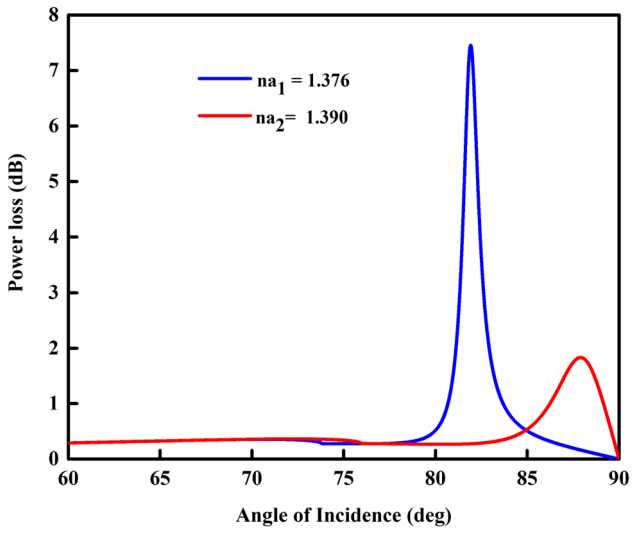

Fig. 5 Power loss vs angle of incidence plot for normal and blood cancerous tissue

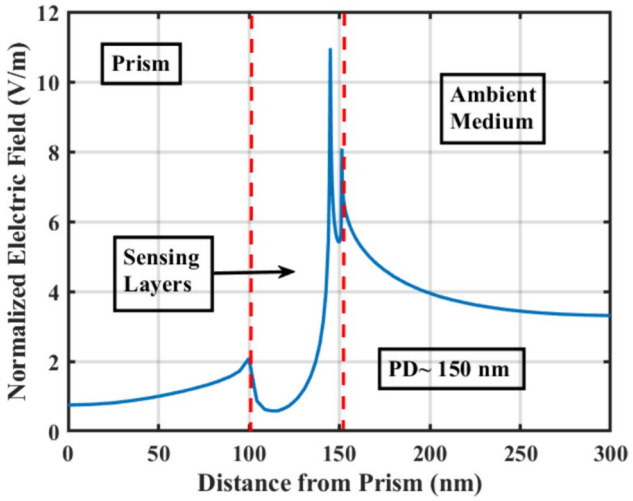

Fig. 6 Normalized electric field plotted against distance for the proposed sensor

combined performance factor (CPF) may be defined as the product of maximum FOM and PLR. Hence, the CPF for the proposed sensor is 882.756 RIU^{-1}.

Figure 6 shows the variation of normalized electric field within the layers of the sensor structure. From the figure, it is clear that the electric field is enhanced due to heterostructure of Ag-Al_2O_3-Ag-graphene. The distribution of electric field plays two roles; It validates the enhancement of electric field due to various layers of the sensor and the ratio of normalized electric field for pathogenic and normal sample at the graphene-analyte interface can be used as performance parameter to realize the sensor close to practicality. Moreover, the long-range sensing of the device is predicted from the penetration depth and field profile in the ambient region. Penetration depth can be defined as distance from the graphene-analyte interface where the normalized field reduces to 1/e of its value at interface. A significant value of normalized field up to a large distance from graphene-analyte interface ensures long-range sensing. The figure suggests the penetration depth of more than 150 nm for the proposed sensor.

Table 3 Comparison of proposed sensor with recently published works on SPR biosensors

Configuration	Sensitivity (deg/RIU)	FOM (RIU^{-1})	Reference
CaF_2/Au/(BP/MoS_2)	252	36.17	[13]
BK7/Ag/BeO/$BaTiO_3$/(BP/WS_2)	360	133.20	[39]
BK7/Ag/ZnO/$PbTiO_3$/BP	365	94.12	[32]
CaF_2/Ag/BeO/Ni/(BP/WS_2)	401.2	178.31	[41]
Present work	427.43	217	-

In the end, a comparison of the presented work with recently published articles based on SPR biosensors has been done, as shown in Table 3.

Conclusion

This study presents an in-depth analysis of a remarkably sensitive biosensor that uses the Surface Plasmon Resonance (SPR) principle for precise detection of the Blood Cancerous cells. In this study, four distinct structures have been explored. Normal and Blood Cancerous tissue have been designated as analytes whose Refractive indices are 1.376 and 1.390 respectively. The thicknesses of the silver, Al2O3, and Ag layers have been optimized in order to achieve the highest possible sensitivity for the sensor. For 45 nm of Ag layer, 1 nm of Al2O3 and again 23 nm of Ag layer, and monolayer of a 2D nanomaterial Graphene at the top, an optimized sensitivity of 427.43 deg/RIU with FoM value of 217 RIU-1 and FWHM of 1.9170 have been accomplished. For the proposed sensor design, plasmon generation and electric field enhancement have also been validated. Consequently, it was inferred that this study could advances the development of a measuring device with remarkable precision and rapid early-stage diagnosis of the blood cancer.

Acknowledgements This work was funded by the Researchers Supporting Project Number (RSP2024R161), King Saud University, Riyadh, Saudi Arabia.

Author Contribution Yashaswini Singh: original draft writing, methodology; Adarsh Chandra Mishra and Sapana Yadav: data analysis and investigation, conceptualization, software work. D. K. Dwivedi, Pooja Lohia, R.K. Yadav, Gaber E. Eldesoky, and M. Khalid Hossain: validation and supervision.

Data Availability The dataset generated during analysis is available in the present article.

Declarations

Ethics Approval This is a theoretical study that does not require ethical approval.

Competing Interests The authors declare no competing interests.

References

1. Tamada K, Li X, Wulandari P et al (2012) Reviews in Plasmonics 2010
2. Yee SS, nter Gauglitz G (1999) Surface plasmon resonance sensors: review
3. Homola J, Yee SS, Gauglitz G (1999) Surface plasmon resonance sensors: review. Sens Actuators B Chem 54:3–15. https://doi.org/10.1016/S0925-4005(98)00321-9
4. Suvarnaphaet P, Pechprasarn S (2017) Graphene-based materials for biosensors: a review. Sensors (Switzerland) 17

5. Fan X, White IM, Shopova SI et al (2008) Sensitive optical biosensors for unlabeled targets: a review. Anal Chim Acta 620:8–26. https://doi.org/10.1016/j.aca.2008.05.022
6. Tian J, Yu S, Yan W, Qiu M (2009) Broadband high-efficiency surface-plasmon-polariton coupler with silicon-metal interface. Appl Phys Lett 95. https://doi.org/10.1063/1.3168653
7. Universitas Prima Indonesia. Fakultas Teknologi & Ilmu Komputer, Institute of Electrical and Electronics Engineers. Indonesia Section. CSS/RAS Joint Chapter, Institute of Electrical and Electronics Engineers MECnIT 2020 : International Conference on Mechanical, Electronics, Computer, and Industrial Technology : June 25–26, 2020, Universitas Prima Indonesia, Medan, Indonesia
8. Uniyal A, Srivastava G, Pal A et al (2023) Recent advances in optical biosensors for sensing applications: a review. Plasmonics 735–750. https://doi.org/10.1007/s11468-023-01803-2
9. Zeng S, Yong KT, Roy I et al (2011) A review on functionalized gold nanoparticles for biosensing applications. Plasmonics 6:491–506. https://doi.org/10.1007/s11468-011-9228-1
10. Shushama KN, Rana MM, Inum R, Hossain MB (2017) Graphene coated fiber optic surface plasmon resonance biosensor for the DNA hybridization detection: simulation analysis. Opt Commun 383:186–190. https://doi.org/10.1016/j.optcom.2016.09.015
11. Shushama KN, Rana MM, Inum R, Hossain MB (2017) Sensitivity enhancement of graphene coated surface plasmon resonance biosensor. Opt Quantum Electron 49. https://doi.org/10.1007/s11082-017-1216-z
12. Singh S, Sharma AK, Lohia P, Dwivedi DK (2021) Ferric oxide and heterostructure BlueP/MoSe2 nanostructure based SPR sensor using magnetic material nickel for sensitivity enhancements. Superlattices Microstruct 107126. https://doi.org/10.1016/j.spmi.2021.107126
13. Singh S, Sharma AK, Lohia P, Dwivedi DK (2021) Sensitivity evaluation of a multi-layered heterostructure blue phosphorene/mos2 surface plasmon resonance based fiber optic sensor: a simulation study. Trans Electr Electron Mater. https://doi.org/10.1007/s42341-021-00344-x
14. Verma A, Prakash A, Tripathi R (2015) Sensitivity enhancement of surface plasmon resonance biosensor using graphene and air gap. Opt Commun 357:106–112. https://doi.org/10.1016/j.optcom.2015.08.076
15. Nur JN, Hasib MHH, Asrafy F et al (2019) Improvement of the performance parameters of the surface plasmon resonance biosensor using Al2O3 and WS2. Opt Quantum Electron 51. https://doi.org/10.1007/s11082-019-1886-9
16. Fitsios D, Alexoudi T, Bazin A et al (2016) Ultra-compact III-V-on-Si photonic crystal memory for flip-flop operation at 5 Gb/s. Opt Express 24:4270. https://doi.org/10.1364/oe.24.004270
17. Verma A, Prakash A, Tripathi R (2015) Performance analysis of graphene based surface plasmon resonance biosensors for detection of pseudomonas-like bacteria. Opt Quantum Electron 47:1197–1205. https://doi.org/10.1007/s11082-014-9976-1
18. Lazcka O, Del CFJ, Muñoz FX (2007) Pathogen detection: a perspective of traditional methods and biosensors. Biosens Bioelectron 22:1205–1217. https://doi.org/10.1016/j.bios.2006.06.036
19. Desu SB, Payne DA (1990) Interfacial segregation in perovskites: III, microstructure and electrical properties. J Am Ceram Soc 73:3407–3415. https://doi.org/10.1111/j.1151-2916.1990.tb06468.x
20. Srivastava A, Das R, Prajapati YK (2020) Effect of perovskite material on performance of surface plasmon resonance biosensor. IET Optoelectron 14:256–265. https://doi.org/10.1049/iet-opt.2019.0122
21. Sadowski JW, Lekkala J, Vikholm I (1991) Biosensors based on surface plasmons excited in non-noble metals. Biosens Bioelectron 6:439–444. https://doi.org/10.1016/0956-5663(91)87009-Z
22. Bhatt S, Bose N, Shushama KN et al (2024) Surface plasmon resonance biosensor with high sensitivity for detecting SARS-CoV-2. Plasmonics. https://doi.org/10.1007/s11468-024-02304-6
23. Chemerkouh MJHN, Saadatmand SB, Hamidi SM (2022) Ultra-high-sensitive biosensor based on SrTiO 3 and two-dimensional materials: ellipsometric concepts. Opt Mater Express 12:2609. https://doi.org/10.1364/ome.457983
24. Karki B, Pal A, Sarkar P et al (2024) Gold, MXene, and graphene nanofilm-based surface plasmon resonance sensor for malaria detection. J Opt (India). https://doi.org/10.1007/s12596-024-01661-z
25. Fouad S, Sabri N, Jamal ZAZ, Poopalan P (2016) Enhanced sensitivity of surface plasmon resonance sensor based on bilayers of silver-barium titanate. J Nano- Electron Phys 8:2–6. https://doi.org/10.21272/jnep.8(4(2)).04085
26. Bai J, Zhou B (2014) Titanium dioxide nanomaterials for sensor applications. Chem Rev 114:10131–10176
27. Singh S, Sharma AK, Lohia P, Dwivedi DK (2021) Theoretical analysis of sensitivity enhancement of surface plasmon resonance biosensor with zinc oxide and blue phosphorus/MoS2 heterostructure. Optik (Stuttg) 244:167618. https://doi.org/10.1016/j.ijleo.2021.167618
28. Umar A, Singh S, Yadav S et al (2022) Numerical study of surface plasmon resonance biosensor using aluminium oxide and bismuth telluride nanomaterials for skin cancer cell detection. 1655–1658. https://doi.org/10.1166/jno.2022.3358
29. Chandra Mishra A, Sharma AK, Lohia P, Dwivedi DK (2024) Silicon nitride (Si3N4) leads to enhanced performance of silica-silver based plasmonic sensor for colorectal cancer detection under optimum radiation damping. Solid State Commun 387. https://doi.org/10.1016/j.ssc.2024.115533
30. Uddin SMA, Chowdhury SS, Kabir E (2021) Numerical analysis of a highly sensitive surface plasmon resonance sensor for SARS-CoV-2 detection. Plasmonics 16:2025–2037. https://doi.org/10.1007/s11468-021-01455-0
31. Saadatmand SB, Ahmadi V, Hamidi SM (2023) Quasi-BIC based all-dielectric metasurfaces for ultra-sensitive refractive index and temperature sensing. Sci Rep 13. https://doi.org/10.1038/s41598-023-48051-2
32. Jaiswal L, Dwivedi DK, Lohia P et al (2024) Numerical study of 2D nanomaterial-based surface plasmon resonance biosensor. Plasmonics. https://doi.org/10.1007/s11468-024-02225-4
33. Singh S, Singh PK, Umar A et al (2020) 2D nanomaterial-based surface plasmon resonance sensors for biosensing applications. Micromachines (Basel) 11. https://doi.org/10.3390/mi11080779
34. Wei W, Nong J, Zhu Y et al (2018) Graphene/Au-enhanced plastic clad silica fiber optic surface plasmon resonance sensor. Plasmonics 13:483–491. https://doi.org/10.1007/s11468-017-0534-0
35. Zeng S, Sreekanth KV, Shang J et al (2015) Graphene-gold metasurface architectures for ultrasensitive plasmonic biosensing. Adv Mater 27:6163–6169. https://doi.org/10.1002/adma.201501754
36. Zeng S, Hu S, Xia J et al (2015) Graphene-MoS2 hybrid nanostructures enhanced surface plasmon resonance biosensors. Sens Actuators B Chem 207:801–810. https://doi.org/10.1016/j.snb.2014.10.124
37. Xu H, Wu L, Dai X et al (2016) An ultra-high sensitivity surface plasmon resonance sensor based on graphene-aluminum-graphene sandwich-like structure. J Appl Phys 120. https://doi.org/10.1063/1.4959982
38. Panda A, Puspa Devi P (2020) Photonic crystal biosensor for refractive index based cancerous cell detection. Opt Fiber Technol 54. https://doi.org/10.1016/j.yofte.2019.102123
39. Singh S, Mishra AC, Singh S et al (2023) Theoretical study of perovskite nano material based surface plasmon resonance biosensor

for cancers cell detection. Optik (Stuttg) 289. https://doi.org/10.1016/j.ijleo.2023.171259
40. Mishra AC, Dandapat K, Tripathi SM et al (2020) Modelling and analysis of chirped long-period grating inscribed in a planer optical waveguide structure for sensing applications. J Opt Commun. https://doi.org/10.1515/joc-2020-0128
41. Mishra AC, Sharma AK, Lohia P, Dwivedi DK (2023) Modelling and analysis of high-performing reconfigurable SPR refractive index sensor employing beryllium oxide, nickel, and BlueP/WS2 nanomaterials. Plasmonics. https://doi.org/10.1007/s11468-023-02005-6
42. Srivastava S, Singh S, Mishra AC et al (2023) Numerical study of titanium dioxide and MXene nanomaterial-based surface plasmon resonance biosensor for virus SARS-CoV-2 detection. Plasmonics. https://doi.org/10.1007/s11468-023-01874-1
43. Shivangani LP, Singh PK et al (2022) Design and modeling of reconfigurable surface plasmon resonance refractive index sensor using Al2O3, nickel, and heterostructure BlueP/WSe2 nanofilms. J Opt (India). https://doi.org/10.1007/s12596-022-00973-2
44. Kaur B, Kumar S, Kaushik BK (2021) 2D Materials-based fiber optic SPR biosensor for cancer detection at 1550 nm. IEEE Sens J 21:23957–23964. https://doi.org/10.1109/JSEN.2021.3110967
45. Singh Y, Dwivedi DK, Lohia P et al (2024) Highly sensitive plasmonic biosensor for the detection of Chikungunya virus employing TiO2 and BP/ws2 heterostructure. Plasmonics. https://doi.org/10.1007/s11468-024-02242-3
46. Srivastava S, Yadav S, Mishra AC et al (2023) Ultra-sensitive surface plasmon resonance biosensor for liver metastases and hepatocellular carcinoma detection using silicon nitride and black phosphorus nanomaterial. Plasmonics. https://doi.org/10.1007/s11468-023-02059-6
47. Sharma AK, Pandey AK, Kaur B (2018) A review of advancements (2007–2017) in plasmonics-based optical fiber sensors. Opt Fiber Technol 43:20–34. https://doi.org/10.1016/j.yofte.2018.03.008